Direct Subangstrom Measurement of Surfaces of Oxide Particles

R. Yu,[1,2,3,*] L. H. Hu,[4] Z. Y. Cheng,[1] Y. D. Li,[3,4] H. Q. Ye,[5] and J. Zhu[1,2,3]

[1]*Beijing National Center for Electron Microscopy, Department of Materials Science and Engineering, Tsinghua University, Beijing 100084, China*

[2]*Laboratory of Advanced Materials, Department of Materials Science and Engineering, Tsinghua University, Beijing 100084, China*

[3]*State Key Laboratory of New Ceramics and Fine Processing, Department of Materials Science and Engineering, Tsinghua University, Beijing 100084, China*

[4]*Department of Chemistry, Tsinghua University, Beijing 100084, China*

[5]*Shenyang National Laboratory for Materials Science, Institute of Metal Research, Chinese Academy of Sciences, Shenyang 110016, China*

(Received 27 August 2010; published 23 November 2010)

Using aberration-corrected transmission electron microscopy combined with first-principles calculations, we show that the surface structure of Co_3O_4, a typical complex oxide, can be directly imaged and quantitatively analyzed at the subangstrom scale. The atomic positions of both light oxygen and heavier cobalt within the surface layers have been measured to an accuracy of several picometers. The surface electronic structure analysis suggests a polarity compensation model based on the electronic polarizability of surface ions.

DOI: 10.1103/PhysRevLett.105.226101 PACS numbers: 68.47.Gh, 68.35.−p, 68.37.Og

Surfaces of metal oxides are of crucial importance for a variety of technological applications such as heterogeneous catalysis, thin film growth, gas sensing, and corrosion prevention [1–3]. Atomic structure and electronic structure of surfaces play important roles in these applications. Especially, chemical reactions and thin film growth on surfaces are atomic processes in nature. The activity and selectivity of catalysts are controlled not only by the atomic configurations, but also by the electronic structure of surfaces [4].

Compared with metals or semiconductors, metal oxides usually have complex crystal structures, allowing a large number of possible surface terminations and corresponding structural modifications. The ionicity and poor conductivity of most metal oxides lead to the formation of surface polarity, which has to be compensated to avoid the electrostatic instability [5]. These complexities present challenges for structural analysis of oxide surfaces by standard surface-science techniques [1,3,6–9]. Therefore, the surface science of oxides lags far behind that of metals and semiconductors.

Conventional surface-science techniques are usually limited to surfaces of single crystals. Surface profile imaging by transmission electron microscopy (TEM) [10] is especially useful for oxide particles [11–13], but had suffered from limited resolution and the delocalization due to aberrations of the objective lens. Recent progress in aberration correction in TEM [14] makes the profile imaging technique a promising method for surface studies of catalysts, as demonstrated for materials of relatively simple structures like Pt and Ag [15–17]. Especially, the structure of surface defects on Pt catalysts, including surface steps and edges, have been quantitatively studied [18]. For complex oxides, however, refined methods with subangstrom resolution are required for genuine atomic imaging and quantitative measurements. Taking spinel-type Co_3O_4 as a model system, here we show that the surface structure of catalytic particles of complex oxides can be directly imaged at the subangstrom scale using aberration-corrected transmission electron microscopy, showing us a powerful tool to exploit novel catalysts urgently needed to solve problems related to energy and environment.

Widely found in materials for technological applications in catalysis and magnetism, the spinel structure is a complex but important structure [19–21]. It has the general formula of AB_2O_4, with oxygen forming a close-packed fcc sublattice, and A and B occupying the tetrahedral and octahedral interstitial sites, respectively. Schematically shown in Fig. 1(a), a conventional unit cell contains eight formular units, giving a total of 56 ions. Because of the structural complexity of the spinel structure, there is more than one possible surface termination depending on the surface orientation. In the [111] direction, the stacking sequence of atomic planes can be described as B_3-O_4-A-B-A-O_4, and thus there are six types of possible (111) surface terminations. Generally, there exist different terminations at different preparation conditions, especially the oxygen partial pressure and the temperature. For example, at least two models for clean (111) surfaces of spinels have been reported. One is terminated with tetrahedral cations [22–25], the other is terminated with octahedral cations [26,27]. Figure 1(b) shows an atomic projection of Co_3O_4 in the close-packed $[1\bar{1}0]$ direction, which is the easiest direction for atom-resolved imaging of the complex material. Tetrahedral and octahedral Co sites are indicated by "T" and "O," respectively. The closest interatomic distance in the projection, 1.1 Å, occurs between oxygen and cobalt columns.

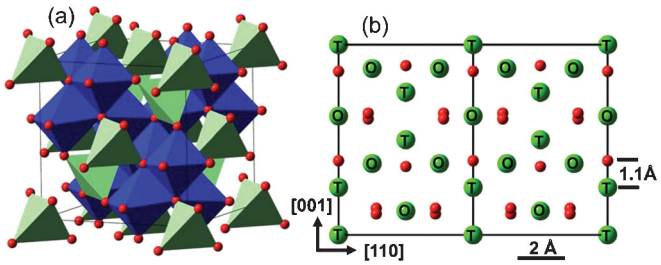

FIG. 1 (color). (a) Schematic unit cell of Co_3O_4 of the spinel structure. The red balls represent the oxygen atoms. The octahedral and tetrahedral sites are occupied by cobalt atoms with valence +3 and +2, respectively. (b) Atomic projection of Co_3O_4 in the close-packed $[1\bar{1}0]$ direction. The cobalt atoms represented by green balls are labeled as *T* and *O*, corresponding to tetrahedral and octahedral sites, respectively.

The Co_3O_4 particles studied in this work were prepared via a hydrothermal process of cobalt hydroxide precursor and subsequent thermal decomposition [28]. The Co_3O_4 nanoparticles were dispersed on carbon-coated copper grids for TEM observations.

High-resolution TEM observations were performed using an FEI Titan 80–300 transmission electron microscope equipped with a spherical aberration (Cs) corrector for the objective lens. The images were taken using the negative-Cs imaging technique, which was shown to give high contrast and low noise [29]. The images were taken at a high tension of 300 kV, with the spherical aberration set at around -13 μm. The other residual aberrations measured before and after image recording are twofold astigmatism $A1 < 2$ nm, threefold astigmatism $A2 < 20$ nm, and coma $B2 < 20$ nm. High-resolution TEM image simulations were carried out using the multislice method [30] as implemented in the MacTempas program. Quantitative measurements of positions of atomic columns were performed by fitting the image areas with intensity maxima to two-dimensional Gaussian functions.

Calculations of the surface structure relaxation were carried out using the projector augmented-wave method [31] within the density functional theory (DFT), as implemented in the VASP code [32,33]. In order to consider correctly the strongly correlated 3*d* orbitals of Co, calculations were performed using the GGA + U approximation [34,35]. Bader's quantum theory of "atoms in molecules" (AIM) [36–38] was employed to analyze the electronic charge redistribution on the polar surface (111) of Co_3O_4. For the (111)-(1 × 1) surface, a hexagonal supercell of 5.756 Å × 5.756 Å × 30.0 Å was used. The supercell contains 55 atoms (24 atomic layers), with a 13.6 Å thick vacuum. More detailed calculation parameters are given in Ref. [38].

Figure 2(a) shows a profile image of the (111) surface of a Co_3O_4 particle viewed along the $[1\bar{1}0]$ direction. A unit cell is outlined by a white rectangle in the center of the image. Compared with the atomic projection shown in Fig. 1(b), the one-to-one correspondence between image intensity maxima and projected atom columns is realized (for more details see Fig. S1 in Ref. [38]). Based on the one-to-one correspondence, the actual surface termination is determined unambiguously to be composed of the Co^{2+} ions occupying the tetrahedral sites, giving Co^{2+}-O_4-Co_3^{3+}-O_4-Co^{2+}-Co^{3+}- for the six outer layers.

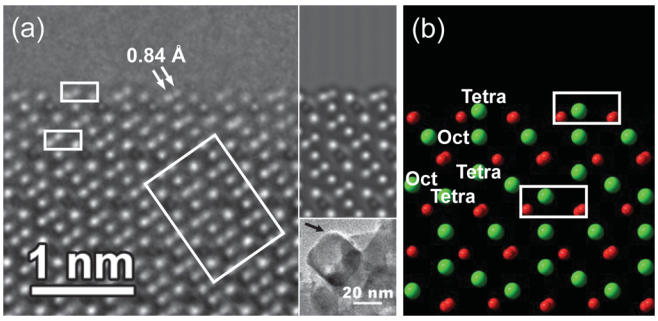

FIG. 2 (color). (a) An experimental subangstrom resolution image of the (111) surface of Co_3O_4. No filtering was applied. The bottom right inset shows an image of the particle at low magnification. (b) Atomic model of the (111) surface of Co_3O_4 relaxed by DFT calculations. The green and red balls represent Co and O atoms, respectively, with tetrahedral and octahedral Co sites labeled. The simulated high-resolution TEM image of the model is shown as an inset in (a), with a thickness of 7.5 nm, an overfocus of 2 nm, and a sample tilt of 2 mrad toward the [001] direction.

A real surface seldom has an ideal structure predicted from the surface termination. Because the bonding situation at the surface is quite different from that in the bulk, a rearrangement of the atoms at and close to the surface usually occurs. Here the structural modification at the surface is quantitatively measured. Imaging and sample parameters are known to affect the locations and intensities of atomic columns in high-resolution TEM images, more sensitively for complex oxides than for materials of simple structures. For example, even a deviation of 0.1° from the zone axis would give a significant change in image contrast for Co_3O_4. Therefore, it is critical to obtain these parameters for the recorded images in order to perform quantitative measurements, even when the experiments have been performed carefully. In this work, these parameters were measured by extensive image simulations and quantitative comparison with the experimental images (see Fig. S2 and Fig. S3 in Ref. [38]). The inset at the top right corner in Fig. 2(a) is a simulated high-resolution TEM image at the measured parameters, which matches well with the experimental image.

In order to facilitate the comparison between the atomic configurations at the surface and inside the crystal, two small rectangles have been drawn in each of Figs. 2(a) and 2(b). As can be seen, the inward relaxation of the top Co^{2+} layer is significant. The atomic positions were measured by fitting the image peaks to two-dimensional Gaussian functions. As labeled in Fig. 2(a), the distance between the cobalt columns in the outermost layer and the oxygen columns in the sublayer is only 0.84 Å, despite the

fact that the distance in the bulk is 1.1 Å. Such small distances between light oxygen columns and heavy metal columns are not uncommon for atomic structures of oxide surfaces, making aberration-corrected TEM with the subangstrom resolution an indispensable tool for surface studies of oxides.

Table I lists the first several spacings between surface atomic planes. Starting from an ideal cleaved surface with the termination (but not the measured relaxation) shown in Fig. 2(a), the surface was relaxed by DFT calculations. The final structure is given in Fig. 2(b). As shown in Table I, the computationally relaxed structure matches the experimental one very well. The outermost layer has contracted by about 50% compared with the bulk. The second spacing (d_2) is also smaller than the corresponding bulk value, while the third spacing (d_3) is larger. Note that the inner spacings have changed to a much less extent (about 10%). Meyer *et al.* [23] have analyzed the surface structure of epitaxial $Co_3O_4(111)$ films on Ir single crystals. In their work, a model similar to the present one gave the best fit between the calculated and experimental LEED spectra. As we noted earlier, the structure of oxide surfaces may vary depending on the preparation conditions. Therefore, surfaces prepared by different methods do not necessarily have similar structure. If they do, however, the excellent agreement between our TEM results and the reported LEED results [23] indicates that the surface structure analysis using subangstrom resolution TEM for small particles can obtain similar accuracy (several picometers) of standard surface-science techniques for single crystals. Furthermore, small changes of inner spacings (d_2 and d_3) can also be determined unambiguously from direct subangstrom TEM measurements.

In heterogeneous catalysis, there is a long-standing problem known as the ''materials gap'': while catalysts are made of small particles, accurate structural information is obtained mostly from single crystals [39]. With the subangstrom measurement technique, it is promising to bridge this ''materials gap'' in catalysis by metal oxides. In particular, surface steps are frequently active sites for heterogeneous catalysis. The determination of their atomic configurations would lead to a deeper understanding of catalysis by oxides. In this regard, the structures of the active sites of Pt catalysts (although not oxides) have been investigated in detail recently by combining aberration-corrected TEM and DFT calculations [18].

TABLE I. Surface relaxation from aberration-corrected TEM, first-principles calculations, and LEED. The surface layers counted from the outermost layer are composed of 1 Co^{2+}, 4 O^{2-}, 3 Co^{3+}, and 4 O^{2-} ions in a surface unit cell, respectively. Spacings (in Å) d_1, d_2, and d_3 denote the first, second, and third spacing between the surface layers, respectively. For the current TEM and DFT study, the spacings at about 2 nm away from the surface are given in parentheses.

Spacings	TEM	DFT	LEED [23]
d_1	0.34 ± 0.09 (0.69 ± 0.05)	0.314 (0.68)	0.32
d_2	0.96 ± 0.04 (1.06 ± 0.06)	0.971 (1.08)	0.95
d_3	1.19 ± 0.05 (1.06 ± 0.05)	1.104 (1.08)	0.99

A critical issue about oxide surfaces is the possible occurrence of polar surfaces and the polarity compensation mechanism [5]. In the case of spinel structure, all the low-index surfaces are polar ones. The polarity compensation mechanism of $Co_3O_4(111)$ surface was discussed by Meyer *et al.* [23] and Vaz *et al.* [24] based on the ionic model. It was shown that additional positive charges are required to compensate the polarity [23,24]. The formation of a surface inversion was suggested by changing the valence state of the outermost Co^{2+} into Co^{3+} ions, providing the additional positive charges to the surface. Based on the accurate geometric structure of the surface, here we calculate surface electronic structure to analyze the polarity compensation mechanism. A clean and stoichiometric surface was assumed in the DFT calculations. The excellent agreement between the experimental and calculated geometrical structure indicates that the adsorption of charged foreign species can be safely ruled out regarding the polarity compensation. The Co^{2+} vacancies could also not be responsible for the polarity compensation, since their presence would result in less positive charges at the surface, in contrast to the requirement for more positive charges. Therefore, the polarity compensation can only be provided by the electron redistribution associated with the structural relaxation. We employ Bader's quantum theory of ''atoms in molecules'' [36] to quantitatively characterize the charge redistribution at the surface. Bader's approach has the advantages of no dependence on basis set selection and of the uniqueness of charge partition.

Fig. 3 shows the calculated Bader charges of the oxygen and cobalt ions as a function of their distance from the surface. A depletion region of electronic charges was observed close the surface, especially for the outer three atomic layers (Co^{2+}-O_4-Co_3^{3+}-). This charge redistribution is equivalent to an increased positive charge at the surface as required for the polarity compensation. As expected from the ionic model, the divalent cations Co^{2+} indeed lost electrons and contribute somewhat to the polarity compensation. However, the trivalent cations Co^{3+} also lost electrons, although to a less extent. More surprisingly, the dominate contribution to the compensation charges originates from the O^{2-} ions, which lost 3 to 5 times more electrons than Co^{2+} and Co^{3+}. This means that the O^{2-} ions, surrounded by a thicker electron cloud, are more vulnerable than Co^{2+} and Co^{3+} for charge redistribution upon the formation of the polar surfaces. This behavior reminds us of the concept of electronic polarizability, the degree to which the electron cloud of an ion is easily polarizable [40]. In fact, the electronic polarizabilities of the Co^{3+}, Co^{2+}, and O^{2-} ions increase in the order of removed electronic charges from the ions. Systematic investigations are needed to establish a quantitative

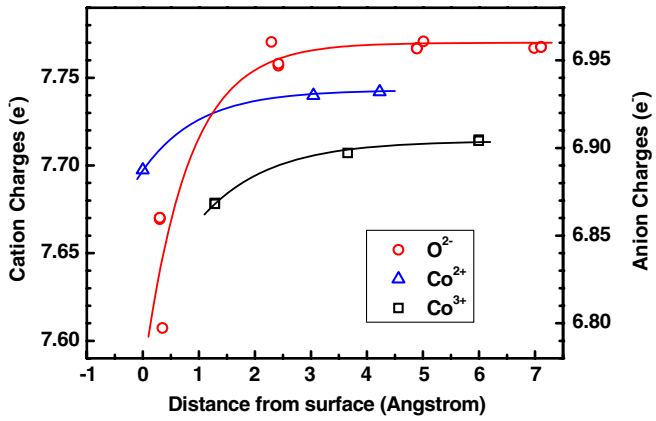

FIG. 3 (color online). Bader charges of the ions as a function of their distance from the surface at 0. Circles: O^{2-}; Triangles: Co^{2+} at tetrahedral sites; Squares: Co^{3+} at octahedral sites. The lines are drawn to guide to the eye.

relationship between the compensation charges of surface ions and their electronic polarizabilities.

In summary, the surface termination, structural relaxation, and electronic structure of the polar (111) surface of complex Co_3O_4 have been investigated quantitatively at the subangstrom resolution by combining aberration-corrected TEM and first-principles calculations. Using the subangstrom measurement technique, it is now possible to attack more effectively problems related to heterogeneous catalysis by metal oxides. In addition to ideal surfaces, structures of surface steps and islands, and their implications for catalysis and thin film growth, are examples that would immediately benefit from these studies.

We thank C. L. Jia and K. Urban for discussions. This work was supported by NSFC (50801040, 90606006, 10979031), the Foundation for the Authors of National Excellent Doctoral Dissertations of China, and the National Basic Research Program of China (2009CB623701, 2006CB932300). This work made use of the resources of the Beijing National Center for Electron Microscopy and Shanghai Supercomputer Center.

*ryu@tsinghua.edu.cn

[1] V. E. Henrich and P. A. Cox, *The Surface Science of Metal Oxides* (Cambridge University Press, Cambridge, 1994).
[2] D. P. Woodruff, *Oxide Surfaces* (Elsevier, Amsterdam, 2001), Vol. 9.
[3] U. Diebold, S.-C. Li, and M. Schmid, Annu. Rev. Phys. Chem. **61**, 129 (2010).
[4] J. K. Norskov *et al.*, Nature Chem. **1**, 37 (2009).
[5] C. Noguera, J. Phys. Condens. Matter **12**, R367 (2000).
[6] G. A. Somorjai, *Introduction to Surface Chemistry and Catalysis* (Wiley, New York, 1994).
[7] K. Takayanagi *et al.*, Surf. Sci. **164**, 367 (1985).
[8] N. Erdman *et al.*, Nature (London) **419**, 55 (2002).
[9] D. A. Bonnell and J. Garra, Rep. Prog. Phys. **71**, 044501 (2008).
[10] L. D. Marks and D. J. Smith, Nature (London) **303**, 316 (1983).
[11] X. G. Ning and H. Q. Ye, Philos. Mag. A **62**, 431 (1990).
[12] D. J. Smith, Rep. Prog. Phys. **60**, 1513 (1997).
[13] J. L. Hutchison and N. A. Briscoe, Ultramicroscopy **18**, 435 (1985).
[14] K. W. Urban, Science **321**, 506 (2008).
[15] L. C. Gontard *et al.*, Angew. Chem., Int. Ed. **46**, 3683 (2007).
[16] D. S. Su *et al.*, Angew. Chem., Int. Ed. **47**, 5005 (2008).
[17] N. Shibata *et al.*, Science **322**, 570 (2008).
[18] L. Y. Chang *et al.*, Nano Lett. **10**, 3073 (2010).
[19] P. A. Cox, *Transition Metal Oxides: An Introduction to Their Electronic Structure and Properties* (Clarendon Press, Oxford, 1992).
[20] C. N. R. Rao and B. Raveau, *Transition Metal Oxides: Structure, Properties, and Synthesis of Ceramic Oxides* (Wiley-VCH, New York, 1998).
[21] S. C. Petitto *et al.*, J. Mol. Catal. A: Chem. **281**, 49 (2008).
[22] M. Ritter and W. Weiss, Surf. Sci. **432**, 81 (1999).
[23] W. Meyer *et al.*, J. Phys. Condens. Matter **20**, 265011 (2008).
[24] C. A. F. Vaz *et al.*, J. Cryst. Growth **311**, 2648 (2009).
[25] X. L. Xu *et al.*, Surf. Sci. **603**, 653 (2009).
[26] J. Ahdjoudj *et al.*, Surf. Sci. **443**, 133 (1999).
[27] C. Lemire *et al.*, Surf. Sci. **572**, 103 (2004).
[28] L. H. Hu, Q. Peng, and Y. D. Li, J. Am. Chem. Soc. **130**, 16 136 (2008).
[29] C. L. Jia, M. Lentzen, and K. Urban, Science **299**, 870 (2003).
[30] J. M. Cowley, *Diffraction Physics* (Elsevier, Amsterdam, 1995).
[31] P. E. Blochl, Phys. Rev. B **50**, 17953 (1994).
[32] G. Kresse and J. Furthmuller, Phys. Rev. B **54**, 11 169 (1996).
[33] G. Kresse and J. Furthmuller, Comput. Mater. Sci. **6**, 15 (1996).
[34] J. P. Perdew, K. Burke, and M. Ernzerhof, Phys. Rev. Lett. **77**, 3865 (1996).
[35] S. L. Dudarev *et al.*, Phys. Rev. B **57**, 1505 (1998).
[36] R. F. W. Bader, *Atoms in Molecules: A Quantum Theory* (Oxford University Press, New York, 1990).
[37] G. Henkelman, A. Arnaldsson, and H. Jónsson, Comput. Mater. Sci. **36**, 354 (2006).
[38] See supplementary material at http://link.aps.org/supplemental/10.1103/PhysRevLett.105.226101.
[39] G. Ertl *et al.*, *Handbook of Heterogeneous Catalysis* (Wiley-VCH, Weinheim, 2008).
[40] C. Kittel, *Introduction to Solid State Physics* (John Wiley and Sons, New York, 2005).